Efficient synergism of concentric ring structure and carbon dots for enhanced methanol electrooxidation

Cong Xiang,‡[a] Yunyun Ling,‡[a] Zitong Zhou,[a] Xiaoyu Zhu,[a] Fan Xue,[a] Zhijun Feng,[a] Yiwei Wang,[a] Xinyi Cheng,[a] Meifang Wang,*[a] and Xiaomei Cheng*[a, b]

[a] *Department of Pharmacy, Wannan Medical College, Wuhu 241002, China*

[b] *State Key Laboratory of Coordination Chemistry, Nanjing University, Nanjing 210023, China*

* Corresponding authors.

E-mail addresses: zijingyuwinter@163.com (M. F. Wang), chengxm@wnmc.edu.cn (X. M. Cheng).

‡ These authors contributed equally to this work.

S1. Experimental section

Tauc's plot is drawn to get the optical bandgap (E_g), for this, we use the following Tauc's relation [S1].

$$(\alpha h\nu)^{\frac{1}{n}} = A(h\nu - E_g) \quad \text{(S1)}$$

where $h\nu$ is the energy of the photon α is the absorption coefficient and E_g is the energy of the material and n is the index (n = ½ for a direct bandgap, and n = 2 for an indirect band). The NiO/Ni-N-CDs0.05 have a direct optical band. The bandgap is obtained from the figure by fitting a plot between $(\alpha h\nu)^2$ versus $h\nu$.

Electrochemically active surface areas (ECSA) were estimated from the electrochemical double-layer capacitance (C_{dl}) based on CVs recorded at different scan rates in the non-faradaic potential range of 0.1-0.2 V *vs.* Ag/AgCl. Plotting the capacitive current (I_c) *vs.* the scan rate (v) yielded a straight line with a slope equal to C_{dl}. ECSA was calculated by dividing C_{dl} by the specific capacitance (C_s) [S2]:

$$ECSA = C_{dl} / C_s \quad \text{(S2)}$$

where C_s is the reported value of 0.06 mF/cm^2 based on the double layer capacitance of an ideal smooth oxide surface.

S2. Figures

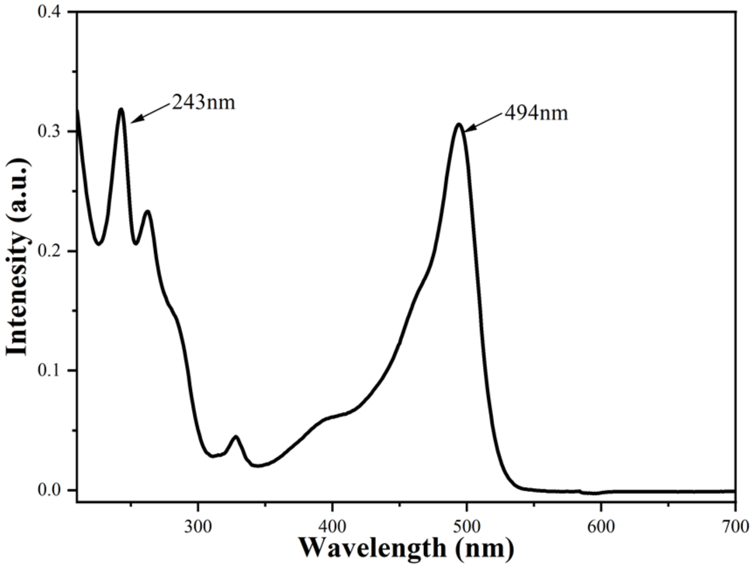

Figure S1. Absorption spectra of N-CDs.

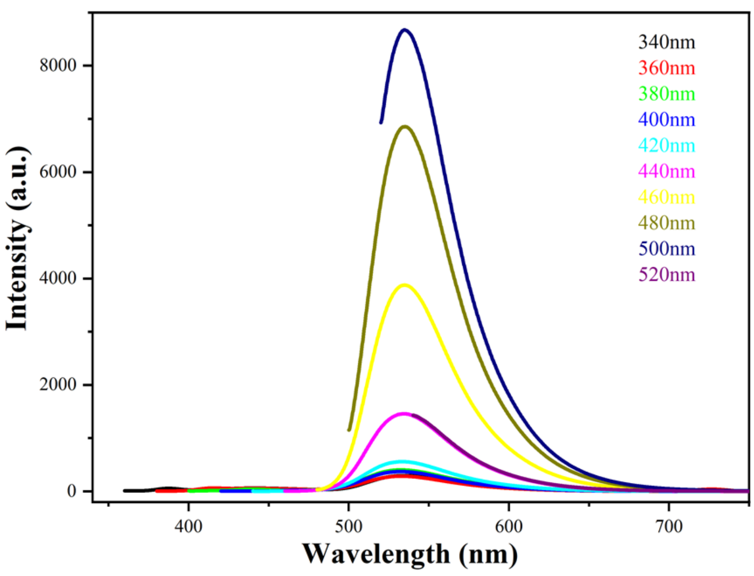

Figure S2. Emission spectra of N-CDs.

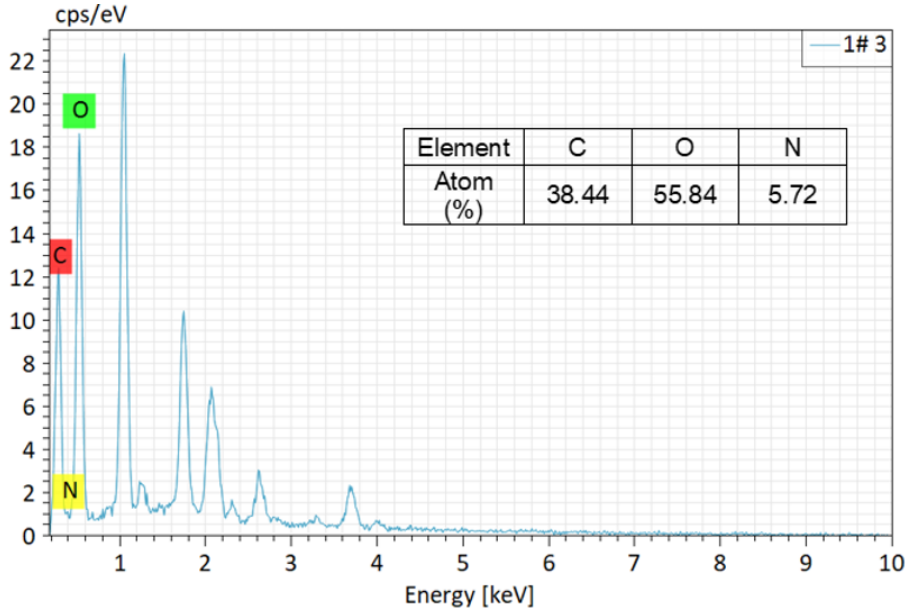

Figure S3. EDS of N-CDs.

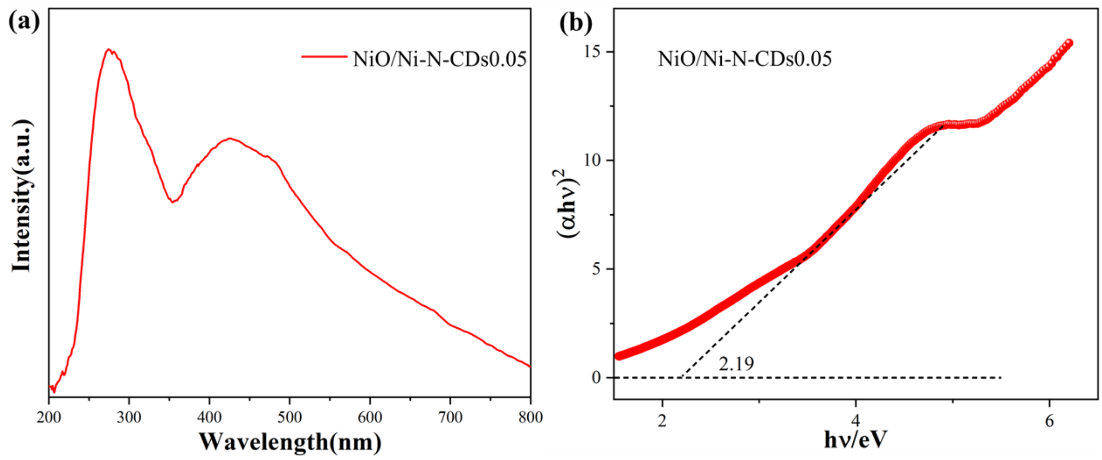

Figure S4. DR-UV-vis absorption spectra of NiO/Ni-N-CDs0.05 (a) Tauc plots (b).

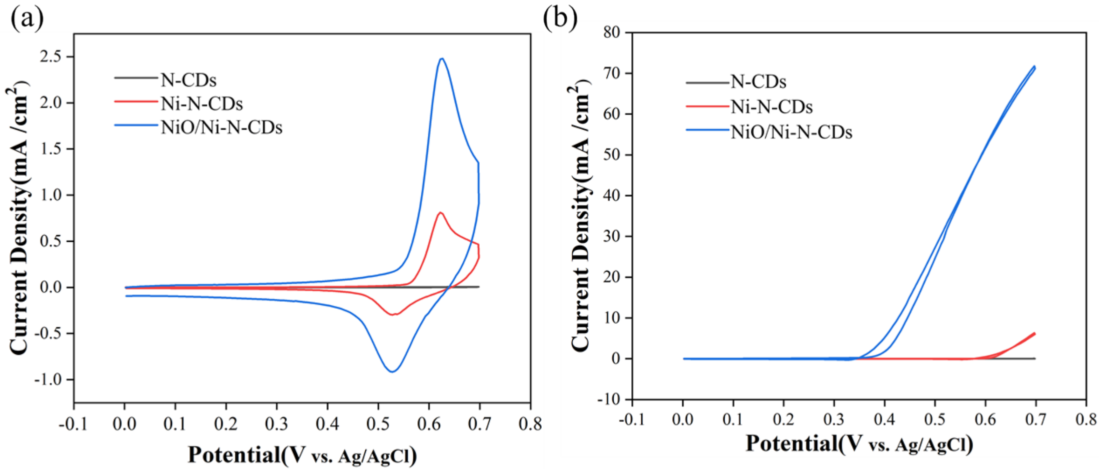

Figure S5. CV curves of Ni-N-CDs, NiO/Ni-N-CDs and N-CDs in (a)1 M KOH and (b) 1 M KOH + 1 M CH_3OH.

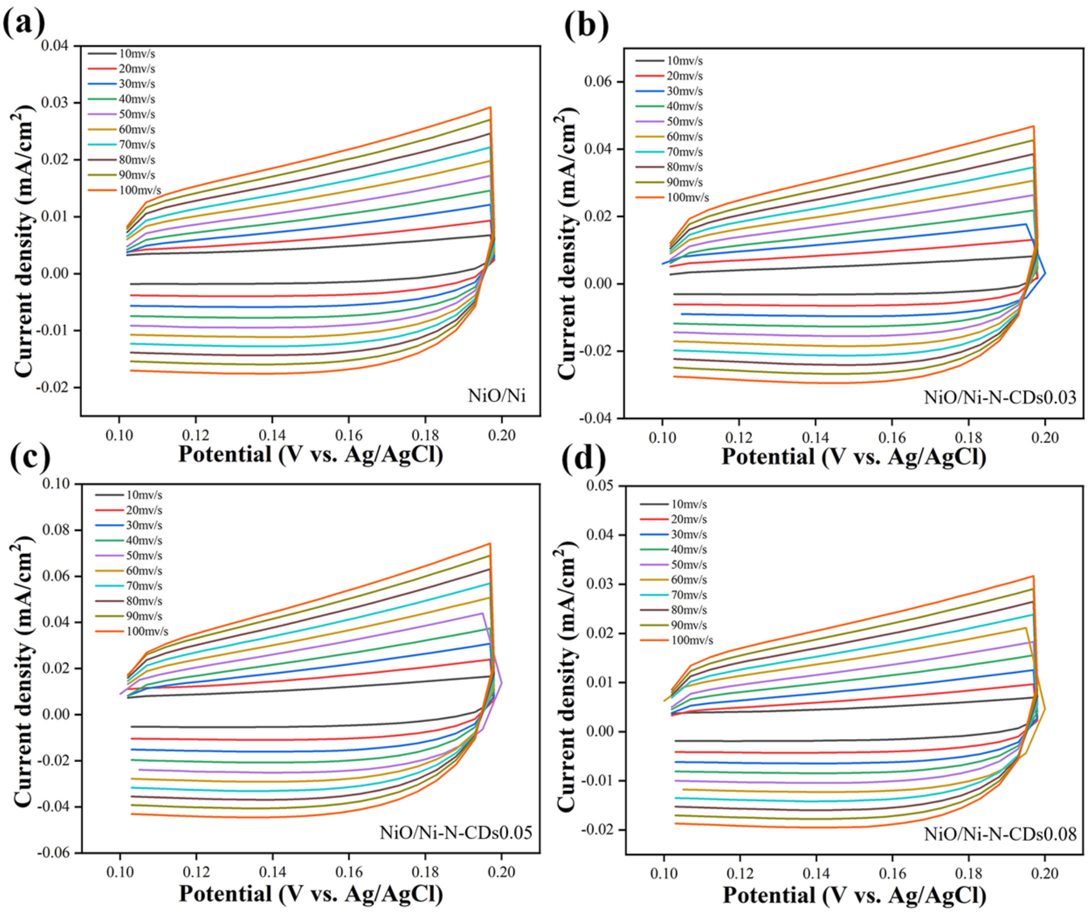

Figure S6. CV curves with different scan rates of (a) NiO/Ni, (b) NiO/Ni-N-CDs0.03, (c) NiO/Ni-N-CDs0.05 and (d) NiO/Ni-N-CDs0.08 in the non-faradaic range of 0.1-0.2V vs.Ag/AgCl.

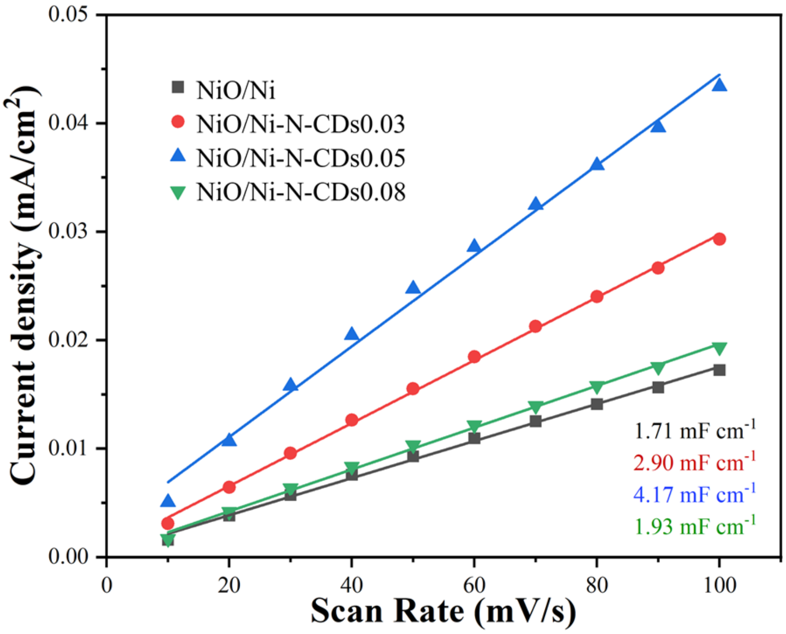

Figure S7. Corresponding linear fit of the capacitive current vs. scan rates to calculate C_{dl}.

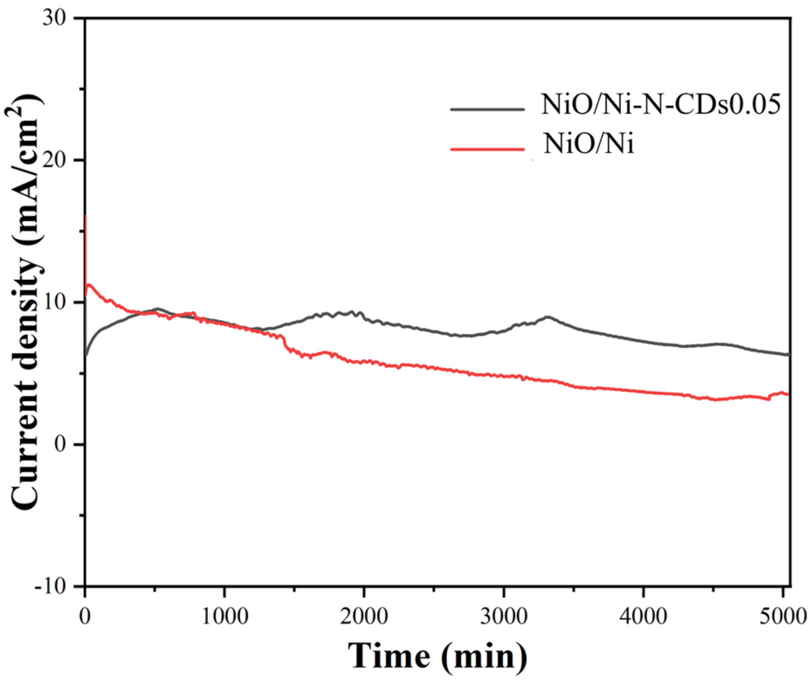

Figure S8. The chronoamperometry curves for all the samples during the MOR.

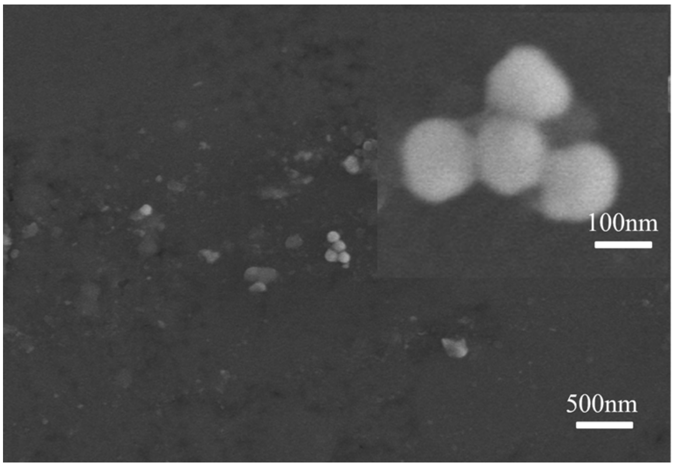

Figure S9. The SEM images of NiO/Ni-N-CDs0.05 after stability test.

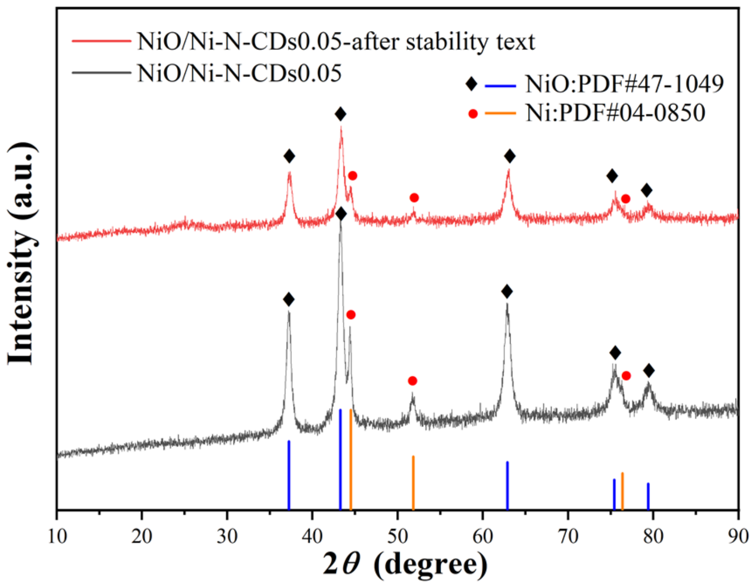

Figure S10. The XRD pattern of NiO/Ni-N-CDs0.05 after stability test.

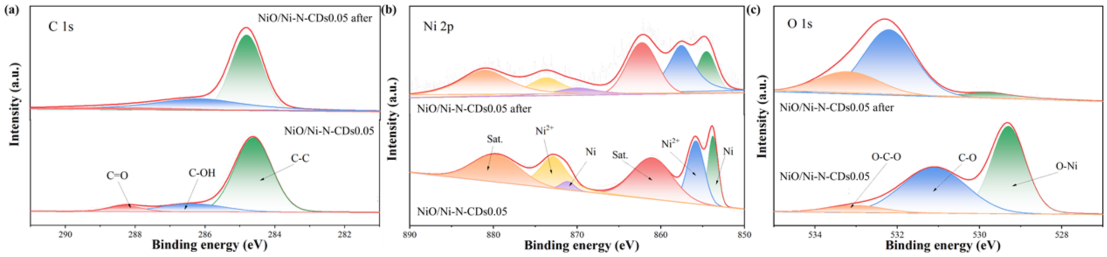

Figure S11. HR-XPS XPS spectra of C 1s (a), Ni 2p (b) and O 1s (c) of NiO/Ni-N-CDs0.05 after stability test.

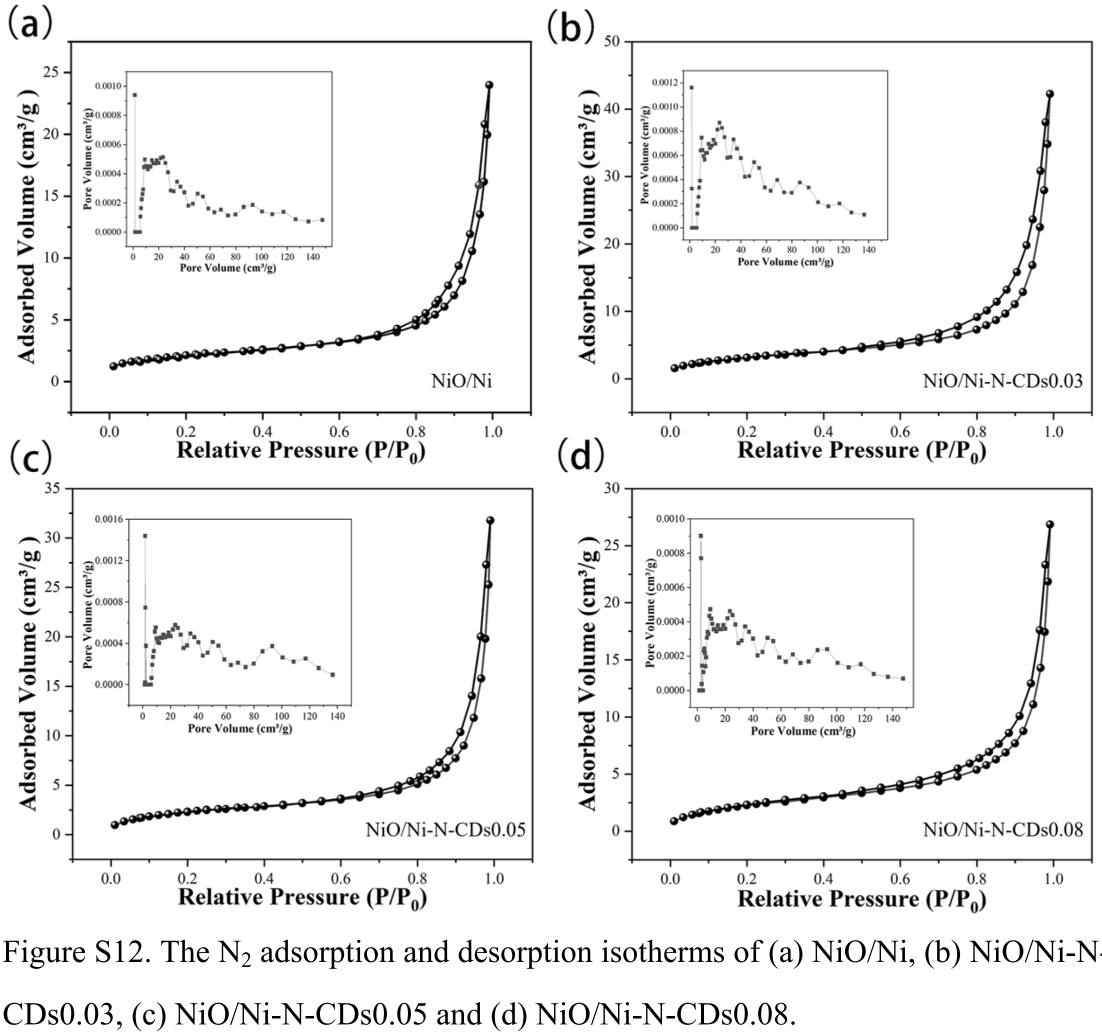

Figure S12. The N_2 adsorption and desorption isotherms of (a) NiO/Ni, (b) NiO/Ni-N-CDs0.03, (c) NiO/Ni-N-CDs0.05 and (d) NiO/Ni-N-CDs0.08.

Table S1. The complete data of the XPS peak fitting of NiO/Ni and NiO/Ni-N-CDs0.05.

		NiO/Ni				NiO/Ni-N-CDs0.05			
Elements	**Peak**	**Position (eV)**	**Area**	**FWHM (eV)**	**%GL**	**Position (eV)**	**Area**	**FWHM (eV)**	**%GL**
C	**C-C**	284.8	18838.4	1.2	18	284.8	199188.6	1.2	10
	C-OH	286.2	3199.1	1.9	51	286.2	4034.4	1.8	55
	C=O	288.4	1532.2	1.5	0	288.4	2010.7	1.2	50
Ni	**Ni^0**	853.2	28287.0	1.1	0	853.2	28011.2	1.1	0
	Ni^0	871.1	9247.1	1.4	0	871.1	10387.4	1.4	0
	Ni^{II}	855.5	71028.8	2.7	0	855.5	72796.3	2.7	0
	Ni^{II}	873.1	53872.1	3.2	63	873.1	56708.8	3.2	63
	Sat.	861.1	96072.1	5.9	0	861.1	94468.4	5.9	0
	Sat.	879.6	73803.7	6.6	5	879.6	71283.2	6.6	0
O	**O-Ni**	529.3	42815.8	0.9	25	529.3	40481.7	1.0	16
	C-O	531.0	28457.0	1.8	0	531.1	34515.4	1.8	0
	O-C-O	533.2	4938.6	2.6	0	533.2	4177.4	1.5	0

Notes and References

[S1] Y. Ding, Y. Chen, M. Wang, Effects of Al incorporation on structural and humidity-sensing properties of SnO_2 sensor, J Mater. Sci. Mater. Electron. 35 (2024) 172. https://doi.org/10.1007/s10854-024-11969-y.

[S2] J. Li, Y. Zuo, J. Liu, X. Wang, X. Yu, R. Du, T. Zhang, M.F. Infante-Carrió, P. Tang, J. Arbiol, J. Llorca, Z. Luo, A. Cabot, Superior methanol electrooxidation performance of (110)-faceted nickel polyhedral nanocrystals, J. Mater. Chem. A 7 (2019) 22036-22043, https://doi.org/10.1039/C9TA07066D.